

Functional Holography of Complex Networks Activity—From Cultures to the Human Brain

ITAY BARUCHI,¹ VERNON L. TOWLE,² AND ESHEL BEN-JACOB^{1,3}

¹School of Physics and Astronomy, Tel Aviv University, 69978 Tel Aviv, Israel; ²Department of Neurology, Surgery, and Pediatric, University of Chicago Hospitals, Chicago, Illinois; and ³The Center for Theoretical and Biological Physics, University of California San Diego, La Jolla, California 92093

Received November 23, 2004; accepted November 23, 2004

A functional holography (FH) approach is introduced for analyzing the complex activity of biological networks in the space of functional correlations. Although the activity is often recorded from part of the nodes only, the goal is to decipher the activity of the whole network. This is why the analysis is guided by the “whole in every part” nature of a holograms—a small part of a hologram will generate the whole picture but with lower resolution. The analysis is started by constructing the space of functional correlations from the similarities between the activities of the network components using a special collective normalization or affinity transformation. Using dimension reduction algorithms like PCA, a connectivity diagram is generated in the 3-dimensional space of the leading eigenvectors of the algorithm. The network components are positioned in the 3-dimensional space by projection on the eigenvectors and connect them with colored lines that represent the similarities. Temporal (causal) information is superimposed by coloring the node’s locations according to the temporal ordering of their activities. Utilizing the analysis, the existence of hidden manifolds with simple yet characteristic geometrical and topological features in the complex biological activity was discovered from cultured networks to the human brain. These findings could be a consequence of the analysis being consistent with a new holographic principle by which biological networks regulate their complex activity. © 2005 Wiley Periodicals, Inc. Complexity 10: 38–51, 2005

Key Words: functional holography; biological networks; similarity matrices; principal component algorithm

1. INTRODUCTION

The activity of complex, multicomponent biological networks is often represented in terms of similarity matrices

and their corresponding connectivity diagrams. Examples range from metabolic pathways, through gene expression, to recorded brain activity. In general, the matrix element $S_{i,j}$ is the computed similarity between the activities of components i and j . The similarity can be based on different measures such as cross-correlations, coherences, and mutual information, depending on the studied net-

Correspondence to: Eshel Ben-Jacob, E-mail: eshel@tamar.tau.ac.il or ebenjacob@ucsd.edu

work. In the case of gene-expression measurements using DNA-microarrays, the similarity is usually the intergene expression correlation [1], whereas in recorded brain activity [e.g., electro-encephalogram (EEG), magneto-encephalogram (MEG), and electrocorticography (ECoG)], it is the interchannel coherences [2].

A common approach in the studies of similarity matrices is to apply clustering algorithms to identify underlying subgroups (clusters) of components that have higher intersimilarities [3]. Many advanced algorithms have been devised according to the specific systems and the assumed motifs that are looked for. In the dendrogram clustering algorithm, for example, the matrices are reordered to place together components with higher similarities. In the principal component algorithm (PCA) and its various variants, like SVD and ICA, the components are projected on a low dimension manifold whose axes are evaluated to capture most of the relevant information in the similarity matrix. The clustering algorithms are based on the implicit notion that the similarity matrices represent a high dimension space of similarities: N -dimension space for a network composed of N components.

Often, the similarity matrices are also visualized by the construction of their corresponding connectivity diagrams, in which a line is drawn between each two component whose similarity is above some threshold. Usually, the lines colors or gray levels represent the level of the similarities. For hard-wired networks (e.g., cultured neural networks), the diagram is constructed according to the components positions in the real network, by placing them on the diagram according to the physical distances. Both for hard-wired networks and distributed networks like gene-networks, the connectivity diagrams can be presented as similarity circles in which the components are placed along a circle and linked with lines that represent the similarities.

In many cases, one can also extract information about the temporal ordering in the activity of the different components, like phase coherences in recorded brain activity or timing between neurons firing in cultured networks [4]. This temporal information can be represented as a temporal ordering matrix whose $T_{i,j}$ describes the relative timing or phase difference between the activities of components i and j .

There has been rapid progress in the fields of data mining and bioinformatics, with new and more advanced visualization approaches and clustering algorithms being continuously developed [5]. Yet, many of the fundamental issues related to the interpretations of the results or, more specifically, the “reversed engineering” from the observed activity to the underlying causes are still to be resolved. The development our method has been motivated by the following goals:

1. To relate the similarity in the activity of two components to their functional dependence.
2. To relate the similarity between two components to the similarity of each with all other components.
3. To compensate for the common limitation incurred by measuring the activity of a fraction of the network components only.
4. To reduce the effect of the inherent noise both in the measurement procedure and in the biological activity itself.
5. To identify underlying simple functional motives in the observed complexity. This quest was motivated by the assumption that such motives must exist if the biological network is to be able to regulate its own complexity.
6. To connect the observed temporal ordering (activity propagation) to underlying causal motives (information propagation and causal connectivity).
7. To identify functional subgroups (functional clusters) and to reveal the functional connectivity between these subgroups.
8. To be able to compare the activity (similarity matrices) of two different networks or different modes of behavior of the same network.

The functional holography (FH) approach is a mathematical concept of visualizing the network in an abstract 3-dimensional space of functional correlations calculated from the similarity matrix. In other words, we construct a dual network by placing the components in the abstract space and linking them according to the similarities. The mathematical procedure involves the following steps:

1. Evaluation of the similarity matrix $S_{i,j}$ between component i and j .
2. Computation of the similarity distances $D_{i,j}$ —the Euclidian distance between the position of components i and j in the N -dimensional space of similarities.
3. Collective normalization of the similarities. The above defined distances are used to normalize the similarities and obtain functional correlations or affinities. That is,

$$A_{i,j} = \frac{C_{i,j}}{D_{i,j}}. \quad (1)$$

In other words, we transform the similarity matrix to a new affinity matrix $A_{i,j}$.

4. Dimension reduction—projecting the N -dimensional affinity space onto a 3-dimensional space that captures the maximal information, using a standard clustering algorithm like PCA (used here), SVD, or ICA. The axes of the space are the three principal eigenvectors of the PCA, and the components position is determined by the

projection of the affinity matrix on these three eigenvectors.

5. Construction of a functional manifold—a connectivity diagram in the 3-dimensional space generated by linking the nodes (component positions) by the original (non-normalized) similarities. In addition (optionally), to capture also the topological properties of the manifold, a curved surface is interpolated between the nodes.
6. Inclusion of temporal (causal) information—the activity propagation on the manifold. When information is available, the temporal ordering matrix is evaluated. The relevant information can be added to the manifold in two ways: (1) Adding arrows to the links between the nodes according to $T_{i,j}$ and (2) evaluating a collective temporal ordering of all the nodes and marking their relative timing by colors or gray levels.
7. Holographic comparison and superposition. The idea is to compare the activity of two networks by projecting the affinity matrix of one network on the PCA leading vectors computed for the other, and vice versa. Two modes of behaviors of the same network may be compared the same way. By superposition, we refer to the projection of each affinity matrix on the mutual PCA leading vectors computed for the combined matrix.
8. Holographic zooming. If we want to magnify a part of the manifold in order to capture more details, simple re-scaling used to magnify a picture will not do. Instead, it is necessary to perform a new iteration of the analysis, starting with a subsimilarity matrix for the cluster of components at the corresponding part of the manifold to be magnified.

The stages (5)–(8) of this functional holography approach are generally applicable to the similarity matrices directly, i.e., they do not depend on the proposed functional normalization. The idea of holographic comparison is expected to be very efficient in many applications, like comparing gene-expression data from different populations of organisms or groups of people.

In the next sections each of the above stages in the FH method is illustrated and described in detail. The recorded spontaneous activities of cultured neural networks are used as a model system to illustrate the power of our new approach in providing a satisfying framework for achieving the goals specified above.

Self-consistency tests of the method to demonstrate its robustness under lesion (reduction in the number of recorded components) and noise tolerance are performed. These tests are discussed in the last section with regard to the rationale behind the functional holography analysis and reasoning why it might provide clues about new self-regulating schemata of biological networks.

Some preliminary results of analyzing ECoG recording of human brain activity during seizure (Ictal) and between

seizure events (inter-Ictal) are presented. In the discussion, it is proposed that the success of the method in capturing the underlying functional and causal motives might imply that the activity of neural networks is self regulated by an underlying simple, low dimension manifolds in the space of functional correlations.

2. EVALUATION OF SIMILARITY MATRICES FOR CULTURED NETWORKS ACTIVITY

Cultured networks provide relatively simple and well-controlled model systems for investigating long term (weeks), individual neurons activity at different locations by using a multielectrode array [6, 7]. The networks whose activity is analyzed here are spontaneously formed from a dissociated mixture of cortical neurons and glia cells from 1-day-old Charles River rats. The cells are homogeneously spread over a lithographically specified area of poly-D-lysine for attachment to the recording electrodes. Consequently, the neurons send dendrites and axons to form a wired network. Although this process is self-executed with no externally provided guiding stimulation or chemical cues, a relatively intense dynamical activity is spontaneously generated within several days. The spontaneous activity of cultured networks is marked by the formation of synchronized bursting events (SBEs), short (~200 ms) time windows, during which most of the recorded neurons participate in relatively rapid firing. The SBEs are separated by long intervals (above seconds) of sporadic neuronal firing. Each SBE can be described as a matrix composed of N vectors, one for each neuron. The vector $X_i(t)$, represents the temporal activity, or firing rate of neuron i , during the time window of the SBE. See Ref. 8 for more details.

To evaluate the interneuron similarity matrix, the Pearson Correlation coefficient [9] is calculated between the bursts of each pair of neurons according to the standard definition:

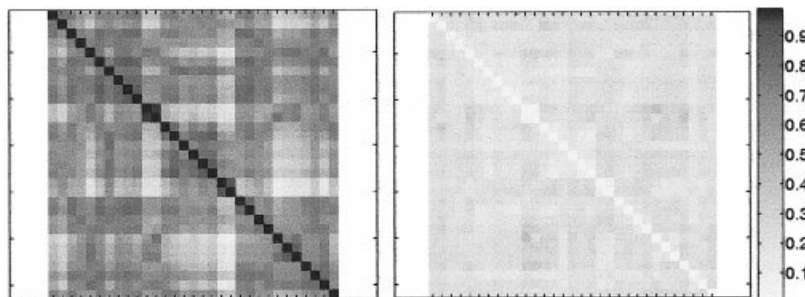
$$C_{i,j} = \frac{\langle (X_i(t) - \mu_i)(X_j(t) - \mu_j) \rangle}{\sigma_i \sigma_j}, \quad (2)$$

where X_i and X_j are the activities of neurons i and j with the corresponding means μ_i and μ_j and sample standard deviations (STD) σ_i and σ_j . The correlation coefficients for all pairs of channels are computed, creating the correlation matrix $C_{i,j}$. Note that, by definition, the correlation matrix is symmetric ($C_{i,j} = C_{j,i}$) and its diagonal is 1 ($C_{i,i} = 1$). Next, the similarity matrix is evaluated by averaging the interneuron correlations over a sequence of SBEs. That is,

$$S_{i,j} = \langle C_{i,j} \rangle_{SBEs}. \quad (3)$$

A typical example of such an interneuron similarity matrix is shown in Figure 1.

FIGURE 1



Left: A typical example of interneuron similarity matrix. Right: The corresponding standard deviation matrix computed as explained in the text. Notice that all STD values are lower than ~ 0.4 and the average is ~ 0.2 .

To test the self-consistency of the above definition, we evaluate a standard deviation matrix whose $STD_{i,j}$ element is the standard deviation of $C_{i,j}$ over the corresponding sequence of SBEs. As can be seen in Figure 1, the deviation is typically smaller than ~ 0.4 and its average is ~ 0.2 . Moreover, using normality tests like the Lilliefors normality test, [10] is obtained. For most pairs of neurons the correlations are distributed normally.

3. THE AFFINITY TRANSFORMATION: COLLECTIVE NORMALIZATION

The similarity matrix of N recorded neurons from a cultured network describes an N -dimension space. The position of neuron i in this space is set by the vector \vec{S}_i —its similarities $S_{i,j}$ with all other neurons j . Accordingly, the similarity distance $D_{i,j}$ between neurons i and j , is simply the Euclidian distance between their positions in the similarity space. That is,¹

$$D_{i,j} = \|\vec{S}_i - \vec{S}_j\| = \sqrt{\sum_{m=1}^N (S_{i,m} - S_{j,m})^2}. \quad (4)$$

As was mentioned in the Introduction, the similarity distances are used for collective or functional normalization of the similarities. The reason the term “collective” is used has to do with the fact that the similarity distance is a functional of the differences between the similarities of the two neurons with the other neurons. The distance is larger if they have different similarities, and vice versa.

The functional normalization, or affinity transformation, is the evaluation of the new affinity or functional correlation matrix defined as follows:

¹Note that in Ref. 4, in the definition of the distances $D(i, j)$ there is division by \sqrt{N} ; both definition are equivalent.

$$A_{i,j} = \begin{cases} \frac{S_{i,j}}{D_{i,j}} & i \neq j \\ A_0 & i = j. \end{cases} \quad (5)$$

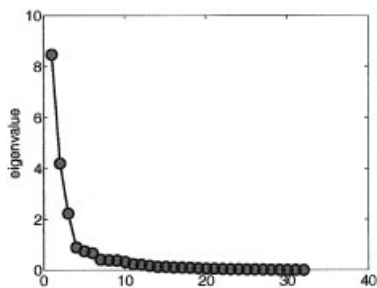
Formally, $D_{i,i} = 0$ and hence the diagonal elements $A_{i,i}$ are ill-defined. However, because of the inherent neuronal plasticity and to noise, there should be uncertainty in the auto-correlation and therefore in the neurons positions in the similarity space. The latter can be translated into position uncertainty and thus into finite $A_{i,i}$, which is related to the effective noise level and neuronal plasticity, and thus has to be properly adjusted to the noise level as will be detailed elsewhere. Here, for simplicity, $A_0 \approx 1/C_0$, where C_0 is taken as the estimated noise level in the neuron correlations.

Since the similarity distances represent a collective property of all channels, the above procedure can help to capture hidden collective motifs related to functional connectivity in the network behaviors.

4. DIMENSION REDUCTION

In the previous section it was mentioned that the similarity matrix can be associated with an N -dimension space in which the neuron i is positioned according to its vector \vec{S}_i . Similarly, the affinity matrix is also associated with an N -dimension space of functional correlations. Correspondingly, the position of neuron i in this space is set by a vector \vec{A}_i —the vector of affinities of this neuron with all other neurons. The analysis is, guided by the assumption that most of the relevant information can be obtained in a low dimension space embedded in the larger one. To test this hypothesis, we evaluate the PCA eigenvalues of an affinity matrix that has been evaluated for the observed activity of a cultured network. The PCA provides a method for identifying new N directions in the N -dimensional space that are ranked (ordered by their eigenvalues) according to the level of standard deviations in the neuron positions [10]. The spectrum shown in Figure 2 indicates that most of the

FIGURE 2



The PCA eigenvalues of an affinity matrix for cultured neural network activity whose similarity matrix is shown in Figure 1. We will refer to this network activity as (I) in the next figures. In this network the number of recorded neurons is $N = 33$. The eigenvalues are for the PCA eigenvectors that are ordered according to the values.

information in the N -dimensional space of the functional correlations can be captured after dimension reduction to a 3-D space whose axes are the three leading PCA eigenvectors. The position of neuron i in this reduced space (X_i, Y_i, Z_i) is set by the projection of \tilde{A}_i on the first three PCA eigenvectors (Fig. 3).

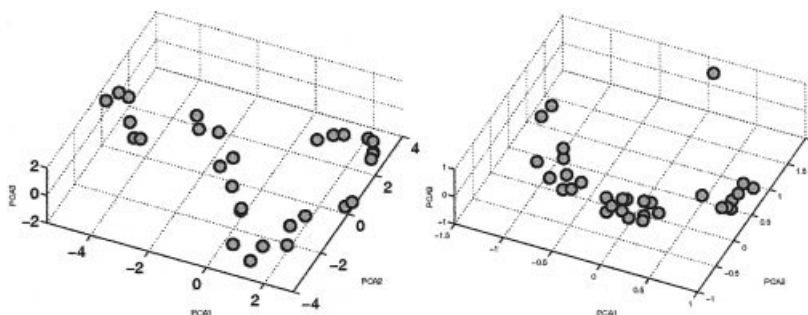
5. FROM CLUSTERS TO MANIFOLDS

Projection of the matrix elements on a low dimensional space (usually 1, 2, or 3), is common in dimension reduction using clustering algorithms. Because the motivation is to look for subgroups or clusters in the collection of components, identification of the clusters is the end result. Guided by the assumption that there are underlying functional manifolds, (stage 5 of our method), the neuron positions are next linked by the “naked” (un-normalized)

similarities above some threshold, as shown in Figure 5. The idea is to add information about inter- and intra-clusters, information that is lost by the projection of the original matrix on its corresponding low dimensional space. The result is a functional connectivity diagram in the abstract space of leading PCA eigenvectors. The term functional is used to emphasize that the diagram includes information about the functional correlations, which determines their position in the diagram. This is to be distinguished from the ordinary connectivity diagrams in which the neurons are positioned according to their physical locations in the network. Interestingly, the strong links (higher levels of similarities) form a bundle with simple geometrical organization and simple yet characteristic topology. The results demonstrate that by bringing back some of the information lost in the dimension reduction we find additional features beyond clustering. Keeping in mind that the recorded neurons are just a small sample of the neurons in the network, we suggest interpolating between the neuron positions according to the similarity links to extract the underlying backbone or the functional manifold of the diagram. It is important to stress that the affinity transformation (the functional normalization) is essential for capturing the hidden manifold—a similar connectivity diagram constructed directly in the 3-D PCA space of the similarity does not show such underlying manifold (Fig. 4).

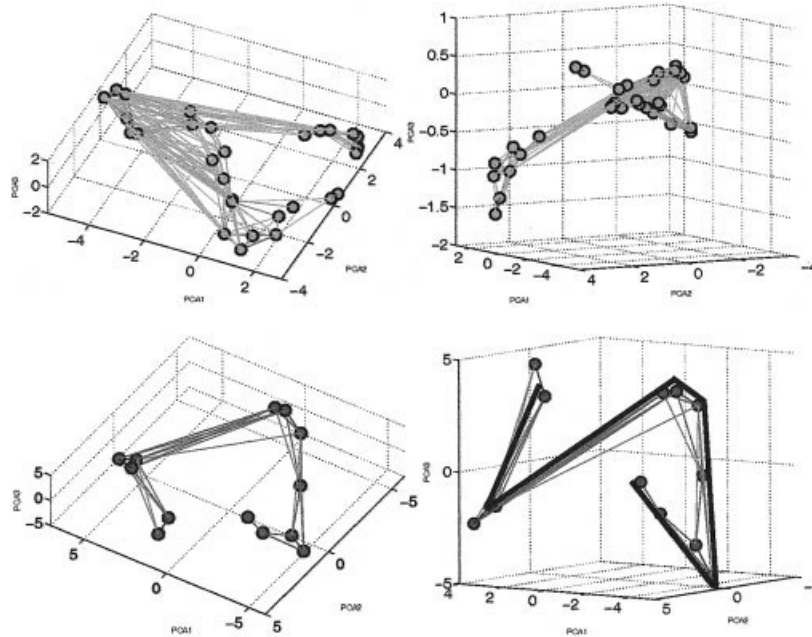
The topology of the manifold of network (II) is that of three perpendicular horseshoes such that the middle one has a joint segment with each of the other two. It is also topologically equivalent to a one turn helix but with a curvature that is not uniform, i.e., it is higher at three specific locations that correspond to the locations of the clusters. It is emphasized that functional manifolds with the same topology, which is simple yet of very specific characteristics,

FIGURE 3



Dimension reduction-projection of the neurons on the 3-D space of the PCA leading eigenvectors of network (I). Left: the projection for the affinity matrix. Right: the projection for the similarity matrix. Comparison of the two figures illustrates the effect of our functional normalization. The projection of the affinity matrix yields a more organized structure. The organization is more pronounced when the neurons are linked by their similarities as is shown in Figure 4.

FIGURE 4



Functional manifolds in the 3-D space of leading PCA eigenvectors. The diagrams at the top show two angles of view of the manifold for network (l) shown in Figure 3. By linking the nodes with similarities (above 0.5) new motifs are revealed, as explained in the text. The most pronounced one is the identification of a quasi 1-D manifold with a specific yet simple topology, as shown in the bottom right figure. The manifold at the bottom left illustrates that this motif is unlikely to be a coincidence as it is exhibited by other networks. The black line is the extracted quasi 1-D manifold (backbone), as explained in the text.

can be identified also in recorded in vivo activity, including from the human brain.

6. FROM MANIFOLDS TO CAUSAL MANIFOLDS

As was mentioned in the introduction, the similarity matrices do not include essential information about the networks behavior: the temporal propagation of the activity relative timing between the components. This additional information (when available) is usually presented in temporal ordering matrices whose $T_{i,j}$ element describes the relative timing or phase difference between the activity of components i and j . There are various methods to evaluate the temporal ordering matrices. In studies of ECoG recorded brain activity, usually it is calculated in terms of “phase coherences”—the relative imaginary parts of the Fourier transform of the activity of channels i and j .

Recently, a new notion—the “temporal center of mass,” or temporal location of each neuron in the SBE time window—was proposed [4]. The idea is to regard the activity density of each neuron i as a temporal weight function so that its temporal center of mass, T_i^n , during a SBE (n) is given by

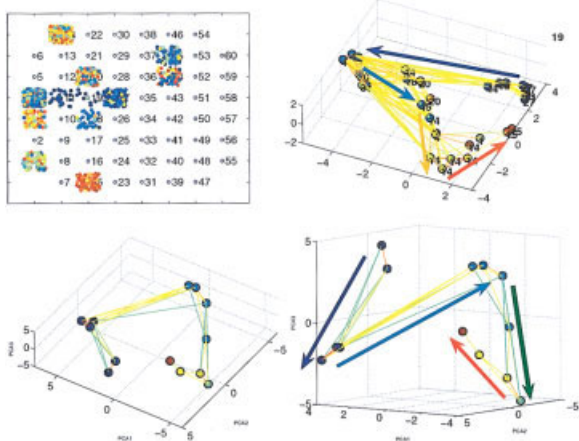
$$T_i^n = \frac{\int (t - T_n) D_i^n(t - T_n) dt}{\int D_i^n(t - T_n) dt}, \quad (6)$$

where the integral is over the time window of the SBE, and T_n marks the temporal location of the n th SBE, which is the combined “center of mass” of all the neurons. As shown in Figure 6, the temporal center of mass of each neuron can vary between the different SBEs. Therefore we define the relative timing of a neuron i to be $T_i \equiv \langle T_i^n \rangle_n$ —the average of the sequence of SBEs. Similarly, we define the temporal ordering matrix as follows:

$$T_{i,j} = \langle T_i^n - T_j^n \rangle. \quad (7)$$

Looking at the activity propagation in real space (Figure 6), it can be seen that it starts in the center of the network near electrodes (11, 19, 27) and propagates in time in two directions—electrodes (3, 4) and (36, 37) to terminate on two opposite sides near electrodes 14 and 15. Interestingly, when the temporal information is superimposed on the

FIGURE 5



Inclusion of the temporal information. Top Left: illustration of the activity propagation in the physical space of the networks. At each neuron position, we mark by gray level the values of its corresponding T_i^j for all the SBEs in the sequence. Top right: illustration of the neuron timing T_i superimposed on the functional connectivity diagram in the 3-D space of leading PCA eigenvectors. The timing is marked by the gray level at the neuron position. Bottom Right: a schematic illustration of the notion about the activity propagation along the quasi-1-D manifold. Bottom Left: an additional example of real network (the one shown in the bottom left picture in Figure 5), with arrows that indicate the temporal ordering added to emphasize the directionality. As one can see, there is clear correspondence between the shape of the manifold, the connectivity of the neurons, and the propagation of the signal. Bottom: more examples of networks that exhibit causality in the affinity manifold.

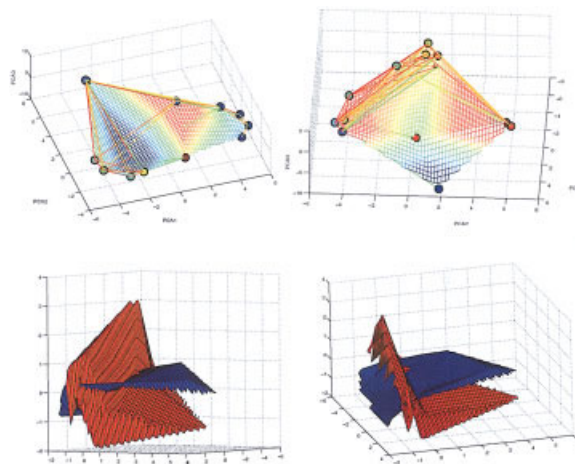
neurons in the 3-D space of leading PCA eigenvectors, the activity propagates along the manifold in an orderly fashion from one end to the other (Figure 6). For this reason, it is proposed to view the resulted manifold, which includes the temporal information as a causal manifold.²

7. HOLOGRAPHIC COMPARISON AND SUPERPOSITION OF NETWORKS ACTIVITY

Often, clustering algorithms are used for comparison between the activities of different networks, e.g., gene-expression in two groups (positive and negative) of patients, or between two modes of behavior of the same network, e.g., during and between epileptic seizures of the same patient.

²In some cases, the functional connectivity diagrams are more complex, and additional visual perception about the causal features of the activity is obtained by interpolation of a curved surface between the neuron positions, as described in Ref. 4. Doing so resulted in a 2-D causal manifold in which the activity propagates mostly along the edges.

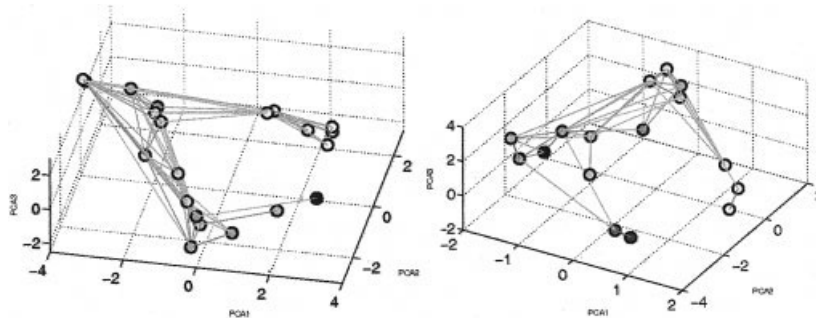
FIGURE 6



Holographic superposition. Large cultured networks exhibit distinct modes of dynamical behavior. This phenomenon is manifested by the observation that the sequence of SBEs is composed of distinct subgroups of SBEs, each with its own characteristic spatiotemporal pattern of activity and interneuron similarity matrix [4, 8]. Top: two manifolds, each for a specific mode of the network activity—a specific subgroup of SBEs. For clarity, we present the manifolds by the 2-D interpolating surfaces. Bottom: the holographic superposition of these two subgroups of SBEs. As described in the text, the similarity matrix for each subgroup is projected on a joint 3-D PCA space. That is a space whose axes are the leading PCA vectors of the combined affinity matrix. As seen, each subgroup generates its own manifold (each has a different gray level). For clarification, for each case we used the 2-D manifold (extrapolation of a curved surface between the nodes). It is also quite transparent that the manifold is intermingled yet perpendicular. We emphasize that each manifold is composed of all the recorded neurons. The holographic superposition makes it possible to enhance the fact that each neuron has different similarities for each subgroup of SBEs. The results shown are for the network analyzed in Refs. 4 and 8.

The following holographic comparison between networks is proposed: (1) Compute the PCA leading eigenvectors of the affinity matrix for each network. (2) Project the affinity matrix of each network on the leading eigenvectors of the other one. This approach can also be used for comparison between different modes of activity of the same networks, like the above-mentioned case of brain activity in between and during seizure. The holographic comparison can also be used to compare different clusters identified in a given matrix. Once the clusters are identified, the similarity matrix for each is isolated from the combined matrix and the above two stages are applied.

The holographic superposition is designed as another method for comparison between different modes of activity of the same network. The idea is similar to the holographic comparison, only the projection is on the mutual PCA leading eigenvectors. That is, the leading eigenvectors of a com-

FIGURE 7

Self-consistency test of lesion robustness. As described in the text, we remove at random several neurons from the recorded information and perform the analysis as if the recorded number of neurons were smaller to begin with. Left: the results of removing 15 neurons out of the original 33. Comparison with Figure 6 reveals that both the characteristic topological features of the manifold and the causal information are retained. It is also important to demonstrate that when large enough fractions of the neurons are removed, the characteristic features eventually washed out. This is demonstrated in the picture on the right, in which 20 neurons were removed. Although the feature of half crescent causal structure is retained, other features begin to wash out.

bined matrix that includes the different modes. In Figure 7 an example of holographic superposition is shown for cultured networks whose activity is composed of distinct subgroups of SBEs (distinct modes of activity).

8. HOLOGRAPHIC ZOOMING

Often, one is interested in more details about a part of the manifold. Such “zooming in” can be performed but not simply by re-scaling of the axes as done, for example, when a part of a picture is magnified. The idea of the holographic zooming is to take advantage of the collective normalization in the following way: (1) Identify the part of the manifold to be magnified, i.e., identify the cluster of relevant component; (2) Isolate the subsimilarity matrix for the cluster; and (3) Perform a second iteration on this matrix, i.e., the affinity transformation, dimension reduction, and construction of a manifold. The latter is the magnified part of the manifold.

As explained in the discussion, the holographic zooming is directly connected to the question about the proper dimension reduction—the proper number of leading PCA eigenvectors to be examined.

9. SELF-CONSISTENCY TESTS OF THE NEW APPROACH

In the Introduction, eight goals were specified that motivated the development of the functional holography approach. The collective normalization fulfils the first two requirements. Stages (6)–(8) in the analysis is designed to provide a satisfactory platform for requirements (6)–(8), respectively, as explained and demonstrated in sections (6)–(8).

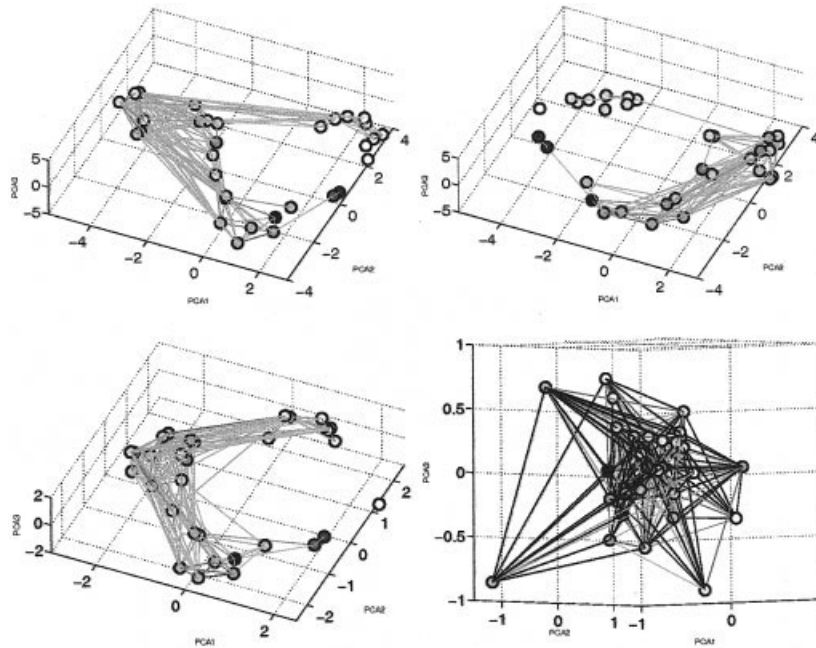
The affinity transformation affords functional holography unique robustness under lesion. This is a crucial self-consistency test of the method. In most cases, the

networks activity is captured by measurements from a number of components that is much smaller than the total number of components in the network. For example, the activity of the cultured neural network is represented by recording from a few tens of neurons out of thousands neurons in the network. The ECoG recorded brain activity is extracted from 64 or 128 locations on the surface of the brain.

To check the method’s lesion robustness, self-consistency tests such as the one shown in Figure 8 were performed. Starting with network i that has 33 recorded neurons; several neurons from the recorded data were randomly removed. As can be seen, even after lesion of 45% of the neurons, both the characteristic topological and causal features of the manifold are retained.

The second feasibility test has to do with the analysis tolerance to noise. As mentioned in the Introduction, the recorded data include noise from different processes, such as inherent biotic noise in the systems, uncontrolled external processes and in the measurement devices. Part of the motivation to use collective normalization was that it can help reduce the effect of noise. Let’s consider two neurons with low functional dependence. The activity of such neurons should have low similarity. In addition, the similarities of each with the other neurons should be very different. Hence they should be positioned far apart in the similarity space (large similarity distance). In the presence of noise, however, it is possible that superficial higher similarity will be detected between them. But, it is very unlikely that noise will have exactly the same effect on the similarities of each of these neurons with all the others so that their similarity distance is reduced. This is why it was expected that normalization by distances would reduce the effect of noise.

FIGURE 8



Testing tolerance to noise. Top: manifolds illustrating the effect of biological-like noise—shifting the spikes by time intervals taken from a normal distribution with standard deviation $\sigma = 10$ ms (left) and $\sigma = 30$ ms (right). Comparison of the manifold in the absence of noise (Figure 6) with the top left one shows that both the topological features and the causal information of the manifold are retained at this high level of noise: the SBE time window is about 100 ms and the average interspike interval is about 10 ms. The top right manifold indicates that for sufficiently high level of noise—when σ becomes comparable with the time width of the SBE—the characteristic features of the manifold are washed out. In the bottom pictures we show the effect of noise that imitates the effect of external noise sources. In this case, noise was added directly to the similarity matrix. The picture on the left is for noise level that is 10% of the averaged similarity. Looking at the shape of the histogram of the similarities, it seems that this level of noise is also comparable with the background noise. As is seen in the left bottom manifold, for this noise level the characteristic features of the manifold are retained. The manifold on the bottom right is when very high noise is added to the correlation matrix so it is almost random. The outcome is an almost random connectivity diagram in the 3-D space.

Two tests were performed. The first is of tolerance to the inherent biological noise. In the case of cultured networks, it is expected to be manifested in small temporal variations in the exact times of the individual neuronal spikes. To check the effect of such inherent temporal biological uncertainties, the noise was imitated by shifting each of the recorded spikes about its temporal location by a small amount picked from a normal distribution. In Figure 9 the analysis is shown to have a very high tolerance to the inherent biological noise.

The method's tolerance to external noise was tested. For that, noise was added directly to the similarity matrix. To estimate what level of noise to add, we plot the histogram of the similarities and take a noise level which is 10% of the averaged similarity. As shown in Figure 9, for such a high level the resulted manifold still retains the characteristic topological and temporal features of the manifold in the absence of additional noise.

The affinity manifold is not only robust to temporal noise but also to correlations noise. In Figure 8 (bottom) the

stability of the manifolds when adding random noise to the correlation matrix is demonstrated. As one can see, distorting the correlation matrix by changing each value $C_{i,j}$ by adding a random number drawn from a Gaussian distribution do not distort the manifold for standard deviations smaller than 0.1.

10. TESTING THE METHOD ON RECORDED HUMAN BRAIN ACTIVITY

In the above sections, we presented examples of manifolds computed for the recorded activity of cultured neural networks. Despite the artificial nature of these networks, the manifolds exhibit simple yet characteristic geometrical and topological features. In an attempt to rule out that these are mere artifacts generated by the method, the recorded activities of chemically stressed networks were analyzed. The results published in Ref. 4 are reassuring: the generated manifolds lost the simple characteristic features of the normal activity. In another, more direct test, a network was dissected into two active networks, revealing that the man-

ifold in the affinity space also split into two. An even more convincing feasibility test of the new method described here involves analysis of recorded human brain activity from epileptic patients who are candidates for brain surgery. The method can also be applied to experimental seizure studies that are gained much attention [11].

The occurrence of epilepsy is rising and is estimated to affect, at some level, 1–2% of the world population [12]. Because of the availability of many anti-epileptic drugs, approximately 80% of all epileptic patients can be kept seizure-free. But for the remaining 20%, the only cure is surgical resection of the seizure focus [13, 14]. One of the most challenging tasks facing epileptologists is precise identification of brain areas to be removed so that the problem can be cured with minimal damage and side effects. Often, the precise location of the epileptogenic region remains uncertain after obtaining conventional, noninvasive measurements such as EEG and MEG can not provide sufficient information because of the relatively low spatial resolution of these methods. In these cases, the activity is directly recorded by the ECoG procedure in which the recording electrodes are placed directly on the brain surface as is shown in Figure 10. The common approach to analyze the ECoG recording is by evaluation of the coherences between each pairs of electrodes. These coherences (the similarities for this case) are the overlap of the Fourier transform of the recorded voltage. Next a connectivity diagrams are constructed and the similarity matrices are analyzed using clustering algorithm as is illustrated in Figure 10. The idea is to compare the resulted connectivity diagrams (or the similarity matrices), during epileptic seizure (Ictal) and between episodes (inter-Ictal) to learn more about the cause of the epilepsy. At present, the functional interpretation of these advanced methods is still not clear especially since the outcome matrices and connectivity diagrams appear more complex than the raw data. Hence, much effort is devoted to improve these methods and to the search for new ones.

In view of the above, the idea that functional holography can reveal the existence of hidden causal manifolds embedded within the complexity of the recorded brain activity was tested, and if so, whether it can also provide an efficient tool to distinguish between the inter-Ictal and the Ictal activities. Typical results are presented in Figure 10. The first four pictures show the manifolds for the similarity matrices in Figure 10. The manifold of the inter-Ictal activity has a very simple topology of almost circular horseshoe like part and another bar perpendicular to its plane and position at the center of the horseshoe. During Ictal the quasi 1-D property of the manifold gives way to a quasi 2-D topology on the surface of a sphere. Albeit the new manifold has more complex topology as could be expected, it retains some of the features of the inter-Ictal one when viewed from specific angle. It hints that the holographic comparison described in

Section 7 might be an efficient method for comparison between the inter-Ictal and Ictal activities as will be described elsewhere.

The horseshoe topology seems to be common both to the cultured networks and the brain activity. In the bottom two pictures in Figure 11 another case (a different patient) is shown in which the recording was from a larger area (a different set of electrodes that covers a larger surface was used). Usually, recording from a larger surface is needed when it is harder to locate the seizure focus or there are multiple foci. The manifold for the larger area recording is composed of two perpendicular manifolds, each with a horseshoe like topology. Using the holographic zooming on one of them reveals that its topology is that of a two perpendicular “Siamese horseshoes” (one joint arm).

The examples above demonstrate the power of the new method to identify hidden motifs in the complex brain activity. Preliminary analyses also indicate that causal features are captured when the temporal (i.e., phase coherences) information is imposed on the manifolds. These results bear the promise that functional holography might become a valuable epileptogenic diagnostic procedure as well as research approach.

11. CONCLUDING REMARKS

A new method for analyzing the complex activity of biological networks is presented, guided by the notion of holograms. In a holographic process, the information describing a 3-D object is encoded on a 2-D photographic film, ready to be regenerated into a holographic image or hologram. A characteristic feature is the “whole in every part” nature of the process: a small part of the photographic film can generate the whole picture, but with fewer details. Another property is high tolerance to noise and high robustness to lesion: even with many imperfections or with several pixels removed, the image of the object as a whole is still retained in the hologram. To magnify a part of the original 3-D object, one needs to produce a new photographic film for the part to be magnified. Another related feature is the holographic superposition—when illuminated together, (placed side by side) two holograms can generate a superposition of the corresponding two 3-D objects. Superposition of objects can also be made by imprinting the images of the two (or more) 3-D objects on the same holographic film. These and other special features of hologram are due to the way the information is encoded on the films—not a direct projection of the picture in real space but in the correlations between the pixels. These are converted back to a picture in three dimensions by proper illumination.

The above properties of holograms guided the development and are the rational behind the functional holography method presented here. The term functional is to indicate that the analysis is in the space of functional correlations that serve the analogue role to the long-range correlations

FIGURE 9

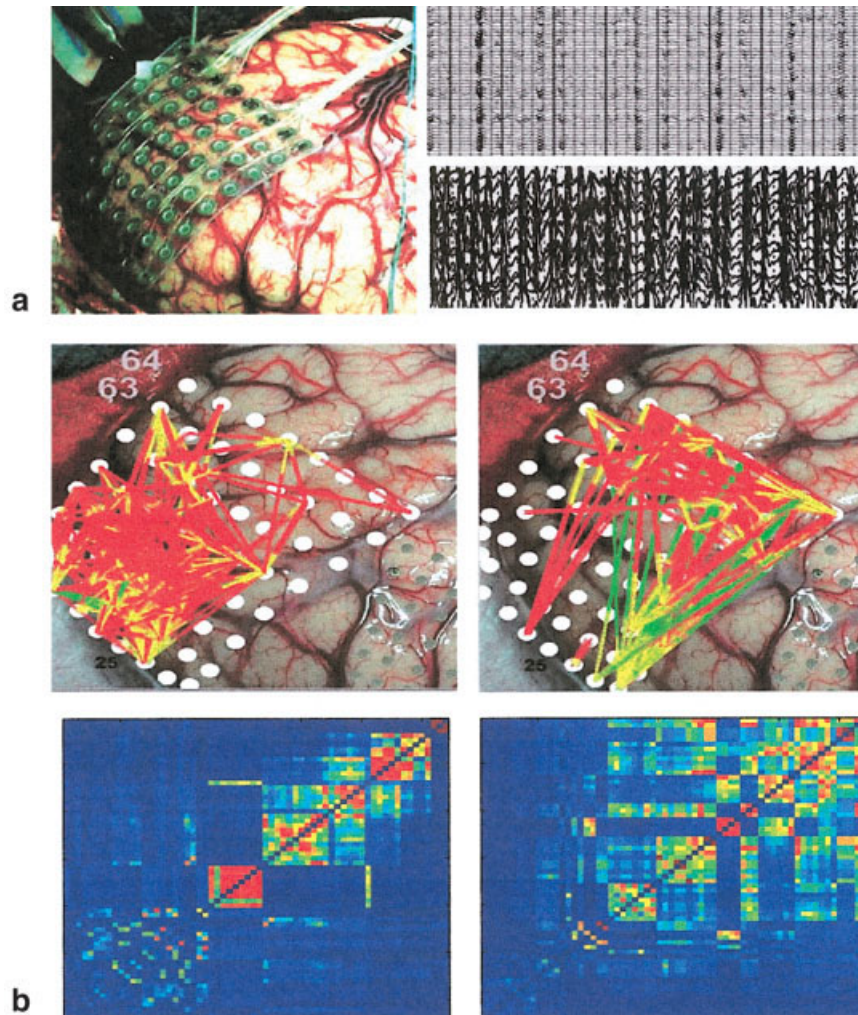


Illustration of the common approach in analyzing ECoG recording of human brain activity. Top left: a set of electrodes placed on the surface of the brain (the frontal lobe in this case). The two pictures in black and white show the voltage recorded from each electrode as function of time. The top one is for inter-ictal activity and the bottom one is for ictal (during seizure). Middle: the connectivity diagram constructed according to the coherences: the color of each link between two electrodes indicate the level of coherence (blue low and red high). The picture on the left is for inter-ictal activity and the one on the right is for ictal. Bottom: the corresponding dendrogrammed similarity matrices. Note that in this case the coherences are used as the measure of the similarities. See Ref. 2 for more details.

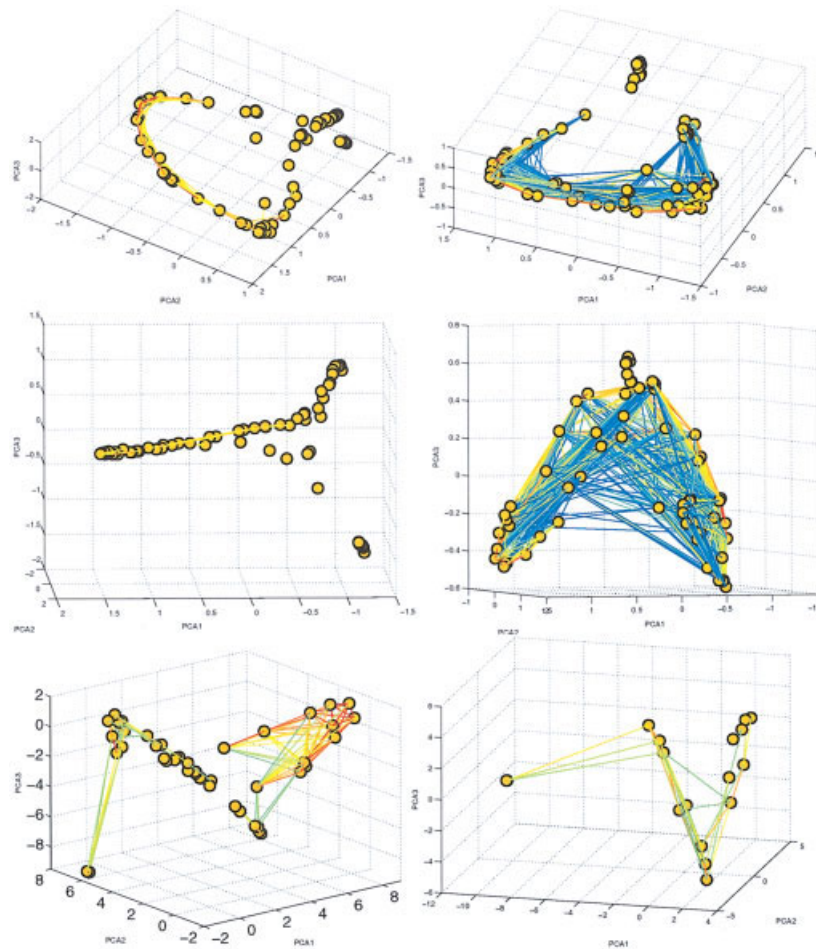
imprinted on the photographic film (by the use of the interference of coherent lights). The methods shown here share the special features of holograms—tolerance to noise, robustness to lesion, holographic superposition, and holographic zooming.

As feasibility tests the method ability to capture hidden motifs in complex activity was used to analyze two extreme examples of neuronal networks: the spontaneous activity of cultured neural networks and recorded human brain activity. In both cases the analyses revealed the existence of hidden low dimension manifolds in the high dimension space of functional correlations. The manifolds have sur-

prisingly simple yet characteristic geometrical topological and causal features. Using holographic superposition different modes of the network activity resulted in an entangled manifold composed of a superposition of the individual modes manifolds. Using holographic zooming on recorded brain activity, we demonstrated how additional hierarchical motifs can be revealed.

The results presented here aimed to demonstrate the potential of the method as a new valuable procedure for diagnosis of biological networks activity. Such diagnostic procedures are needed for the interpretation of recorded brain activity using EEG, MEG, ECoG, and fMRI [15]. For

FIGURE 10



Examples of causal manifolds for ECoG recorded human brain activity. The top four pictures are for the inter-ictal and ictal activities shown in Figure 10. The ones on the left are for inter-ictal and those on the right are for ictal. For each case we show the manifold from two angles of view. The bottom pictures show the holographic zooming for a different set of recordings from a different patient. The recordings in this case were from a larger area. The similarity in this case was calculated by evaluation of the correlations between the voltage traces from each electrode. Note that the manifold shown on the left picture is composed of two perpendicular horseshoes like manifolds. The picture on the right shows a holographic magnification of the left one. The magnification reveals that this manifold is also composed of two perpendicular horseshoe but with a joint leg.

example, the purpose of ECoG is to localize a suspected seizure focus in the cerebral cortex for patients who are candidates for surgery. The decision of whether to remove or to leave a marginally active area of cortex intact elicits a wide range of opinions from clinicians. Although it is expensive and manpower intensive, ECoG remains the cardinal method for determining the anatomic site of seizure onset, yet even this method of direct recording is not always conclusive. When the seizures involve the medial temporal lobe or are associated with a demonstrable neoplastic process, surgery is successful in about 60–70% of cases. However, when the seizures are suggestive of extra-temporal foci, or no lesion can be identified by MRI and fMRI, the success rate of surgical interven-

tions drops precipitously to less than 50%. This poor cure rate for extra-temporal seizure implies that the current conceptualizations about the disorder are inadequate [16–18], and more accurate models of epileptic processes and better diagnostic procedures are needed. As was mentioned earlier, functional holography might provide satisfactory solution to this need.

To further test the general applicability of the method, preliminary analysis of recorded spinal activity from lamprey was performed, of fMRI measurements of human brain activity and of DNA-microarrays measurements of gene-expression. Again, hidden manifolds with simple geometrical and topological features are discovered. These results give rise to some intriguing questions.

Although can not be ruled out, it is unlikely that they are just accidental. Assuming they are not, they can still be a consequence of some inherent artifact of the method itself. To test that this is not the case we applied the method to analyze the activity of simulated networks whose structure of synaptic connectivity and the nature of neurons (e.g., inhibitory vs. excitatory), are controlled [19, 20]. The method can identify, for example, the inhibitory neurons and the existence of subnetworks when the network is composed of overlapping ones. The efficiency of the method was also tested in comparison between modeled and real networks and found that it can identify additional self-regulation motives in the real ones.

Clearly, additional detailed tests of the method on a variety of systems are needed, but let assume that the discovered hidden causal manifolds are real rather than accidental or arbitrary. The most fundamental question then is why it is so effective. It is proposed that the reason is that the analysis is consistent with the manner in which the biological networks regulate their complex activity. In Ref. 21 it was shown that even for cultured neural networks the activity is self-regulated to operate at maximal complexity.

Higher complexity is proposed to afford the network with elevated plasticity to perform a wide spectrum of tasks [4, 21–23]. Motivated by the above it is proposed that the holographic principle for the self-regulation of the networks complex activity. The basic assumptions are as follows: (1) that the networks activity is performed and regulated in the space of functional correlation. For neural networks it implies that the information is processed (encoded decoded and computed) in functional correlations rather than in rates or timing. (2) These high dimension space is regulated by hierarchically organized low dimension manifolds with simple geometry and topology. The hierarchical organization is according to the holographic zooming described earlier. (3) The different modes of behavior and the activity of different subnetworks are mutually regulated by the holographic superposition which keeps entangled yet perpendicular manifolds, and (4) holographic creativity and a continuous space of manifolds. Using a discrete set of photographic films it is possible to generate a continuous spectrum of holograms that are constructed by different combinations of the photographic films with continuous adjustment of the relative illumination. In an analogous manner the biological networks can create new modes of behaviors from a discrete set of fundamental subnetworks each with its own manifold.

Biological networks do not have photographic films to store holograms nor do they have illuminating lights to for imprinting and regeneration. Hence one can doubt the possible reality of the above holographic principle beyond being just an intellectual metaphor. Indeed, as will be explained in detail, for the principle to be relevant to biological networks the activity must be regulated by at least two complementary mechanisms like the glia regulation in neural networks [24–26]. Simply phrased, neuro-glia fabrics provide the “photographic films” for the holograms, which can be imprinted and retrieved by calcium and other chemical waves regulated by the glia cells when act as excitable media.

If correct, the holographic schemata provide the brain with an entirely new ways of coding decoding and processing of information. For example, to sustain associative memory what is needed is the equivalent of superposition of two small portions of the photographic films of each memory. The most attractive is that the holographic schemata provides in principle simple solutions to the fundamental question of creation new images or new meanings of texts. These can be sustaining by the holographic superposition and holographic creativity.

ACKNOWLEDGMENTS

The method presented here has evolved from the joint study with Dr. Ronen Segev, Eyal Hulata, and Yoash Shapira [7]. Much insight has been gained from analyzing the activity of cultured networks in collaboration with Vladislav Volman and from analyzing the structure of artificial and neural networks in collaboration with Pablo Blinder and Dr. Danny Baranes. One of us (E.B.-J.) is most thankful to Prof Steven Schiff for many illuminating conversations, guidance into the foundations and the literature about epilepsy and constructive comments and advice during the development of this research. We thank Prof. Robert Benzi, Prof. Eytan Domany, Prof. Sir Sam Edwards, Prof. Herbert Levine, Dr. John Hunter, and Prof. Itamar Procaccia for constructive comments about the mathematical basis of the method. Preliminary analyses of fMRI measurements are done in collaboration with Dr. Talma Handler and Dr. Yaniv Asaf. This research was partially supported by a grant from the Israel Science Foundation, the Maguy-Glass chair in Physics of Complex Systems, and National Science Foundation Grant PHY 99-07949. One of us (E.B.-J.) thanks the K.I.T.P. at University of California Santa Barbara, the Weitzman Institute and the Center for Theoretical and Biological Physics for hospitality during various stages of this research.

REFERENCES

1. Ihmels, J.; Levy, R.; Barkai, N. Principles of transcriptional control in the metabolic network of *Saccharomyces cerevisiae*. *Nature Biotechnol.* doi:10.1038/nbt918 (2003).
2. Vernon, L.T.; Syed, I.; Bergera, C.; Grzesczukb, R.; Miltona, J.; Ericksonc, R.K.; Cogenc, P.; Berksona, E.; Spirea, J.P. Identification of the sensory/motor area and pathologic regions using ECoG coherence. *Electroencephalog Clin Neurophysiol* 1998, 106, 30–39.
3. Brazier, M.A.B. *Cluster Analysis*; London: Edward Arnold, 1993; p 256.
4. Baruchi, I.; Ben-Jacob, E. Functional holography of recorded neuronal networks activity. *Neuroinformatics* 2004, 2(3), 333–352(20).
5. Hoffman, P.E.; Grinstein, G.G. *A survey of visualizations for high-dimensional data mining*. Morgan Kaufmann Publishers, 2002; pp 47–82.
6. Kamioka, H.; Maeda, E.; Jimbo, Y.; Robinson H.P.C.; Kawana, A. Spontaneous periodic synchronized bursting during formation of mature patterns of connections in cortical cultures. *Neurosci Lett* 1996, 206, 109–112.
7. Segev, R.; Benveniste, M.; Hulata, E.; Cohen, N.; Palevski, A.; Kapon, E.; Shapira, Y.; and Ben-Jacob, E. Long term behavior of lithographically prepared in vitro neuronal networks. *Phys Rev Lett* 2002, 88, 118102.
8. Segev, R.; Baruchi, I.; Hulata, E.; Ben-Jacob, E. Hidden neuronal correlations in cultured networks. *Phys Rev Lett* 2004, 92, 118102.
9. Otnes, R.K.; Enochson, L. *Applied Time Series Analysis*; Wiley Interscience, 1978.
10. Conover, W.J.; *Practical Nonparametric Statistics*; Wiley: New York, 1980; Krzanowski, W.J. *Principles of Multivariate Analysis—A User's Perspective*; Oxford University Press, 1990.
11. Netoff, T.; Schiff, S.J. Decreased neuronal synchronization during experimental seizures. *Neuroscience* 2002, 22, 7297–7307.
12. Towle, V.L.; Ahmad, F.; Kohrman, M.; Hecox, K.; Chkhenkeli, S. *Electrocorticographic Coherence Patterns of Epileptic Seizures in Epilepsy as a Dynamic Disease*; P. Jung, P.; Milton, J., Eds.; Springer: Berlin, 2002.
13. Doyle, W.K., Spencer, D.D. Anterior temporal resections. In: *Epilepsy: A Comprehensive Textbook*; Engel, J., Jr.; Pedley, T.A., Eds.; Vol. 2. Lippincott-Raven, 1998; pp 1807–1817.
14. Chkhenkeli, S.A.; Towle, V.L.; Milton, J.G.; Spire, J.-P. Multitarget stereotactic surgery of intractable epilepsy. In: *Abstr. of the XIII Congress of ESSFN*. Freiburg, Germany. 1998; 4:21.
15. Bandettini, P.A.; Moonen, C.T.W.; Aguirre, G. K. *Functional MRI*, 1st Ed.; Springer-Verlag Telos: July 15, 1999.
16. Bickford, R.G. The application of depth electroencephalography in some varieties of epilepsy. *Electroencephalogr Clin Neurophysiol* 1956, 8, 526–527.
17. Brazier, M.A.B. Evoked responses from the depths of the human brain. *Ann NY Acad Sci* 1964, 112, 33–59.
18. Brazier, M.A.B. Spread of seizure discharges in epilepsy: Anatomical and electrophysiological considerations. *Exp Neurol* 1972, 36, 263–272.
19. Volman, V.; Baruchi, I.; Persi, E.; Ben-Jacob, E. Generative modeling of regulated activity in cultured neuronal networks. *Physica A* 2004, 335, 249–278.
20. Volman, V.; Baruchi, I.; Ben-Jacob, E. Self-regulated homoclinic chaos in neural networks activity. *8th Experimental Chaos Conference* (in press).
21. Hulata, E.; Baruchi, I.; Segev, R.; Shapira, Y.; Ben-Jacob, E. Self-regulated complexity in cultured neuronal networks. *Phys Rev Lett* 2004, 92(19), 198105(1–198105(4)).
22. Ben-Jacob, E. Bacterial self-organization: Co-enhancement of complexification and adaptability in a dynamic environment. *Phil Trans R Soc Lond A* 2003, 361, 1283–1312.
23. Ayali, A.; Fuchs, E.; Zilberstein, Y.; Shefi, O.; Hulata, E.; Baruchi, I.; Ben Jacob, E. Contextual regularity and complexity of neuronal activity: From stand-alone cultures to task-performing animals. *Complexity* Vol. 9, 2004, 6, 25–32.
24. Stevens, B.; Porta, S.; Haak, LL.; Gallo, V.; Fields, R.D. Adenosine: A neuron-glia transmitter promoting myelination in the CNS in response to action potentials neuron. *2002*, 36, 855–868
25. Laming, P.R.; Kimelberg, H.; Robinson, S.; Salm, A.; Hawrylak, N.; Müller, C.; Roots, B.; Ng, K. Neuronal-glia interactions. *Behav Neurosci Biobehav Rev* 2000, 24, 295–340.
26. Stout, C.E.; Constantin, J.L.; Naus, C.G.; Charles, A.C. Intercellular calcium signaling in astrocytes via ATP release through connexin hemichannels. *J Biol Chem* 2002, 277, 10482–10488.